JOURNAL OF VIROLOGY, June 2007, p. 5561–5572 Vol. 81, No. 11
0022-538X/07/$08.00+0 doi:10.1128/JVI.01857-06

A Phylogenetically Conserved RNA Structure in the Poliovirus Open Reading Frame Inhibits the Antiviral Endoribonuclease RNase L▽

Jian-Qiu Han,[1] Hannah L. Townsend,[1] Babal Kant Jha,[3] Jayashree M. Paranjape,[3] Robert H. Silverman,[3] and David J. Barton[1,2]*

Department of Microbiology[1] and Program in Molecular Biology,[2] University of Colorado, School of Medicine, Aurora, Colorado 80045, and Department of Cancer Biology, The Lerner Research Institute, The Cleveland Clinic Foundation, Cleveland, Ohio 44106[3]

Received 25 August 2006/Accepted 26 February 2007

RNase L is an antiviral endoribonuclease that cleaves viral mRNAs after single-stranded UA and UU dinucleotides. Poliovirus (PV) mRNA is surprisingly resistant to cleavage by RNase L due to an RNA structure in the $3C^{Pro}$ open reading frame (ORF). The RNA structure associated with the inhibition of RNase L is phylogenetically conserved in group C enteroviruses, including PV type 1 (PV1), PV2, PV3, coxsackie A virus 11 (CAV11), CAV13, CAV17, CAV20, CAV21, and CAV24. The RNA structure is not present in other human enteroviruses (group A, B, or D enteroviruses). Coxsackievirus B3 mRNA and hepatitis C virus mRNA were fully sensitive to cleavage by RNase L. HeLa cells expressing either wild-type RNase L or a dominant-negative mutant RNase L were used to examine the effects of RNase L on PV replication. PV replication was not inhibited by RNase L activity, but rRNA cleavage characteristic of RNase L activity was detected late during the course of PV infection, after assembly of intracellular virus. Rather than inhibiting PV replication, RNase L activity was associated with larger plaques and better cell-to-cell spread. Mutations in the RNA structure associated with the inhibition of RNase L did not affect the magnitude of PV replication in HeLa cells expressing RNase L, consistent with the absence of observed RNase L activity until after virus assembly. Thus, PV carries an RNA structure in the 3C protease ORF that potently inhibits the endonuclease activity of RNase L, but this RNA structure does not prevent RNase L activity late during the course of infection, as virus assembly nears completion.

RNase L is a latent endoribonuclease in an interferon-regulated and double-stranded RNA (dsRNA)-activated antiviral pathway (reviewed in reference 47). Although RNase L is expressed in most human cells, it becomes active only after viral dsRNA accumulates and provokes the synthesis of 2′-5′ oligoadenylate (2-5A) by 2′-5′ oligoadenylate synthetases (2-5 OAS) (18, 64). 2-5A binds to ankyrin repeats within the N terminus of monomeric RNase L, provoking conformational changes which lead to RNase L dimerization and activation of endoribonuclease activity (20, 21, 57). The endoribonuclease of RNase L cleaves RNAs predominantly after single-stranded UA and UU dinucleotides (22, 62). Viral mRNAs like that of hepatitis C virus (HCV) are exquisitely sensitive to cleavage by RNase L in vitro (26, 27). Reduced frequencies of UA and UU dinucleotides within the open reading frames (ORFs) of HCV mRNAs are consistent with the selective pressure of RNase L. Activated RNase L also cleaves cellular RNAs, including rRNA (61). rRNA cleavage characteristic of activated RNase L is associated with the synthesis and accumulation of viral dsRNA during the course of infections (6, 16, 52, 55).

RNase L is thought to manifest antiviral activity via two independent mechanisms, namely, by cleaving viral RNA and by promoting apoptosis (65). Poliovirus (PV) infection activates apoptotic pathways; however, PV also delays apoptotic death to accommodate the time needed for viral replication (1, 2, 49, 58). The mechanisms by which PV activates and delays apoptotic death are poorly defined.

We report the discovery of an RNA structure in the PV ORF that potently inhibits the endoribonuclease activity of RNase L. Furthermore, we report that RNase L activity late during the course of PV replication did not diminish virus production. Rather, RNase L activity was associated with larger plaques and increased cell-to-cell spread. We discuss the ironic possibility that PV coopts an interferon-regulated and dsRNA-activated antiviral pathway, perhaps in concert with other dsRNA-activated pathways, to mediate the cytopathic effect (CPE) and virus release.

MATERIALS AND METHODS

Viral RNAs. Full-length viral RNAs were synthesized by the use of T7 polymerase (Epicentre, Madison, WI) from plasmids carrying cDNAs of PV (5, 51), coxsackievirus B3 (CVB3) (12), and HCV (36) linearized with the following restriction enzymes: MluI for PV, ClaI for CVB3, and MluI for HCV. PV M1123, a virus with nine wobble position mutations, was engineered using the following primers encoding the mutations: M1123+, 5′ GGTACAAGGACCAGGGTTC GATTACGCAGTGG 3′; and M1123(−), 5′ CGAGCAGTTTGGCGCCCAC CGAGATTTAGATAACCTTGTTCCGTGACTGCCCCCACCGGTAC ATAC 3′. The PCR product containing the mutations was cut with BglII and KasI and inserted into the corresponding region of full-length PV cDNA. DNA sequencing was used to confirm the integrity of PV M1123. Fragments of PV RNA were synthesized by T7 transcription, using PCR-generated templates encoding the appropriate portions of PV. When necessary, ^{32}P[CTP] (Amersham) was added to reaction mixtures to make radiolabeled RNA. Viral RNAs were precipitated with 2.5 M ammonium acetate, pH 7.0, washed with ethanol, solubilized in water, and quantified by the UV absorption at 260 nm.

* Corresponding author. Mailing address: Department of Microbiology, School of Medicine, University of Colorado, Mail Stop 8333, Room P18-9116, 12800 E. 19th Ave., Aurora, CO 80045. Phone: (303) 724-4215. Fax: (303) 724-4226. E-mail: david.barton@uchsc.edu.

▽ Published ahead of print on 7 March 2007.

RNA cleavage using purified RNase L and 2-5A. RNase L and 2-5A were purified as previously described (50, 54), with modifications. Briefly, untagged recombinant human RNase L in a baculovirus vector was expressed in SF21 insect cells. Suspension cultures of SF21 cells were grown in SFM 900 insect cell medium (Invitrogen) supplemented with 10% fetal bovine serum to a cell density of 1.5×10^6 to 2.0×10^6 cells/ml. Cells were infected at a multiplicity of infection (MOI) of 5 PFU per cell at 27°C for 72 h before being harvested. The cell pellets were washed with chilled phosphate-buffered saline (PBS), resuspended in lysis buffer (20 mM HEPES, pH 7.4, 5 mM $MgCl_2$, 50 mM KCl, 1 mM EDTA, 10% glycerol, 14 mM 2-mercaptoethanol [2-ME], 100 μM ATP, 20 μg/ml leupeptin, 20 μg/ml pepstatin, 50 μM phenylmethylsulfonyl fluoride [PMSF]), and disrupted with a French press. Supernatants were collected after centrifugation at $100{,}000 \times g$ and incubated for 1 hour at 4°C with CL6B Blue Sepharose affinity resin (Amersham Bioscience). The protein-bound affinity resin was packed in an HR16/24 column and washed with buffer A (20 mM HEPES, pH 7.4, 5 mM $MgCl_2$, 50 mM KCl, 1 mM EDTA, 10% glycerol, 7 mM 2-ME, 100 μM ATP, 2 μg/ml leupeptin, 2 μg/ml pepstatin, 50 μM PMSF). The bound RNase L was eluted with a 0 to 100% linear gradient of buffer B (20 mM HEPES, pH 7.4, 5 mM $MgCl_2$, 1.0 M KCl, 1 mM EDTA, 10% glycerol, 7 mM 2-ME, 100 μM ATP, 2 μg/ml leupeptin, 2 μg/ml pepstatin, 50 μM PMSF) over a period of 1 h at a flow rate of 1 ml/min. The peak fractions containing RNase L were pooled, dialyzed against four changes of buffer A, loaded onto a MonoQ HR 10/10 column, and eluted with a 0 to 50% buffer B gradient over a period of 60 min at a flow rate of 1 ml/min. The purity of RNase L was >90%, as judged by sodium dodecyl sulfate (SDS)-polyacrylamide gel electrophoresis followed by Coomassie blue staining. 2-5A was synthesized from ATP with recombinant porcine 2-5 OAS (a generous gift of R. Hartmann, Cleveland Clinic) activated with poly(I) · poly(C) linked to agarose beads, purified with a fast-performance liquid chromatography MonoQ column (HR 10/10), and characterized by high-performance liquid chromatography on a Dionex P100 analytical column. RNA cleavage reaction mixtures (10 to 50 μl) containing 100 nM ^{32}P-labeled viral RNA, 5 to 40 nM RNase L (as indicated), 5 to 40 nM p_3A_3 2-5A (as indicated), 25 mM Tris-HCl (pH 7.4), 100 mM KCl, 10 mM $MgCl_2$, 50 μM ATP, and 7 mM 2-ME were incubated at 25 to 30°C. Fragments of PV RNA were included in reaction mixtures to inhibit RNase L, as indicated in the figure legends. Reactions were terminated by adding 100 to 250 μl SDS buffer (0.5% SDS [Sigma], 10 mM Tris-HCl, pH 7.5, 1 mM EDTA, 100 mM NaCl). RNAs from the reactions were precipitated with ethanol and separated by electrophoresis in 1% agarose gels containing MOPS (morpholinepropanesulfonic acid)-formaldehyde buffer and 0.1 mg/ml ethidium bromide. RNAs within gels were visualized using UV light or detected by phosphorimaging.

HeLa cells expressing wild-type or DN RNase L. HeLa M cells were stably transfected with pcDNA3 vectors to establish the following three related cell lines: a cell line overexpressing wild-type RNase L (W12 HeLa cells), a cell line overexpressing RNase L with a dominant-negative (DN) R667A mutation (M25 HeLa cells), and control HeLa cells carrying vector alone (V11 HeLa cells). Cells were grown in Dulbecco's modified Eagle's medium (DMEM; Invitrogen) containing 10% fetal bovine serum (HyClone, Logan, UT), 250 μg/ml G418 (Sigma, St. Louis, MO), 100 U per ml penicillin, and 1,000 U per ml streptomycin (HyClone, Logan, UT).

PV infections and plaque assays. PV type 1 (Mahoney; PV1) was grown and titrated in HeLa M cells. An MOI of 5 to 10 was used for one-step growth experiments. HeLa cells (5×10^5) were seeded in 35-mm plates 18 to 22 h before infection. Cells were infected with virus diluted in 200 μl DMEM. Following 1 h of adsorption at 37°C, the inoculum was removed and replaced with 3 ml of DMEM containing 10% fetal bovine serum, penicillin, and streptomycin. G418 (250 μg/ml) was included in the medium when pcDNA3 vectors were present within HeLa cells. Total virus was harvested in the medium at the indicated times after three cycles of freeze-thawing cells. Plaque assays were similar except that infected cells were overlaid with 2 ml of medium containing 10% fetal bovine serum, penicillin, streptomycin, and 1.2% methylcellulose (Sigma, St. Louis, MO). After 2 to 3 days of incubation, methylcellulose overlays were removed, and cell monolayers were fixed with 5% trichloroacetic acid and stained with a solution containing 0.2% crystal violet, 2% ethanol, and 0.08% ammonium oxalate.

Western blotting. Cells were infected as described above. At the indicated times, cells were rinsed with PBS and solubilized with 250 μl of radioimmunoprecipitation assay buffer (150 mM NaCl, 1.0% Igepal CA-630, 0.5% sodium deoxycholate, 0.1% SDS, 50 mM Tris, pH 8.0). Two hundred fifty microliters of 2× Laemmli buffer was added, and samples were boiled at 95°C for 5 min. A 20-μl sample was fractionated by electrophoresis in a 9% SDS-polyacrylamide gel, and proteins were transferred to a polyvinylidene difluoride membrane (Amersham). Polyclonal rabbit antibodies against OAS1 (Abgent, San Diego, CA), a mouse monoclonal antibody against human RNase L (Novus Biologicals), and a monoclonal antibody to actin (Sigma) were used along with chemiluminescence, as described by the manufacturer (ECL Plus; Amersham), to detect proteins.

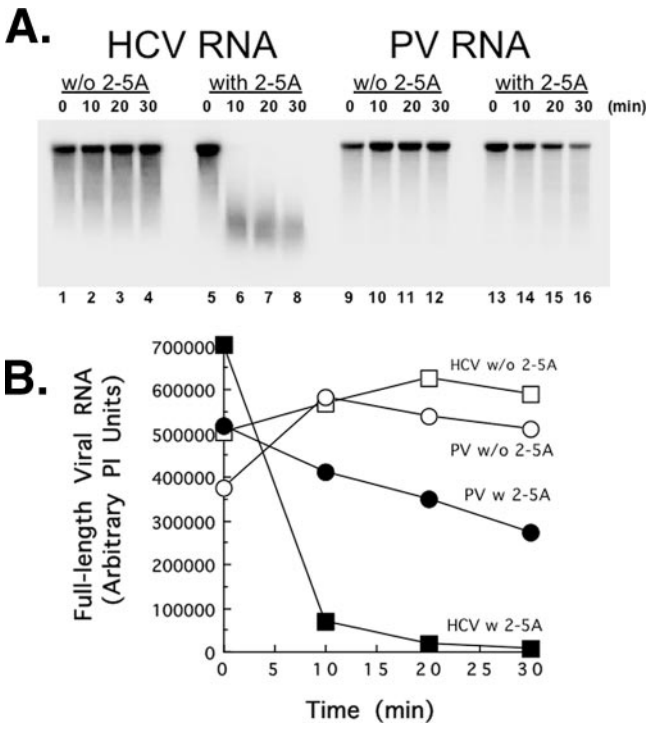

FIG. 1. PV RNA resists cleavage by RNase L. ^{32}P-labeled HCV and PV RNAs (100 nM) were incubated for 0 to 30 min at 25°C in reaction mixtures containing RNase L (10 nM) in the absence or presence of 2-5A (10 nM), as indicated. RNAs separated by electrophoresis in 1% agarose were detected by phosphorimaging (A), and relative amounts of intact RNA were plotted versus time (B). PI units, phosphorimaging units.

Total cellular RNA and rRNA cleavage in PV-infected cells. Cells were infected as described above. The medium was removed at the indicated times postinfection. Monolayers were rinsed with PBS and solubilized with 1 ml SDS buffer (0.5% SDS [Sigma, St. Louis, MO], 10 mM Tris-HCl, pH 7.5, 1 mM EDTA, 100 mM NaCl). Samples were extracted with phenol-chloroform, ethanol precipitated, solubilized in 40 μl water, and treated with 2 units of DNase in 1× DNase buffer (Epicenter, Madison, WI) for 15 min at 37°C. Following DNase treatment, total cellular RNA was precipitated with ethanol, fractionated by electrophoresis in 1% agarose-MOPS gels (~250,000 cells per lane), stained with ethidium bromide, and visualized by UV light.

RESULTS

PV RNA is resistant to cleavage by RNase L. PV RNA has 112 UA and UU dinucleotides per kb of ORF, while HCV 1a RNA has only 73 UA and UU dinucleotides per kb of ORF. Because RNase L cleaves viral RNAs at single-stranded UA and UU dinucleotides, we predicted that PV RNA would be cleaved by RNase L more readily than HCV RNA.

Contrary to our prediction, PV RNA was quite resistant to cleavage by RNase L (Fig. 1). We used purified RNase L, purified 2-5A, and viral RNAs made from cDNA clones to assay viral RNA cleavage by RNase L (Fig. 1). HCV and PV RNAs were perfectly stable in reaction mixtures containing purified RNase L without 2-5A (Fig. 1A, lanes 1 to 4 and 9 to 12). This result is consistent with the requirement of 2-5A for

activation of RNase L and demonstrated that other 2-5A-independent nucleases were not present in the reaction mixes. In the presence of 2-5A, RNase L cleaved HCV RNA into fragments of 200 to 1,000 nucleotides (nt) (Fig. 1A, lanes 5 to 8). Surprisingly, PV RNA was not cleaved by RNase L more readily than HCV RNA was (Fig. 1A, compare lanes 5 to 8 with lanes 13 to 16). Less than 50% of the 7.5-kb PV RNA molecules were cleaved at all during the 30-min incubation (Fig. 1B). This result was striking because PV RNA has hundreds of UA and UU dinucleotides as potential RNase L cleavage sites.

A phylogenetically conserved RNA structure in the 3C^{Pro} ORF inhibits 2-5A-activated RNase L. Based on the results presented in Fig. 1, we speculated that PV RNA might contain an RNA sequence or structure capable of inhibiting RNase L. We further speculated that such a sequence or structure would most likely reside in the 5′- and/or 3′-nontranslated regions (NTRs) of PV RNA rather than the viral ORF because the 5′ and 3′ NTRs contain phylogenetically conserved *cis*-active RNA structures (60). As illustrated in Fig. 2A, PV RNA contains a 5′ NTR, one long ORF, a 3′ NTR, and a poly(A) tail. DJB14 RNA is an engineered subgenomic PV RNA from which most of the viral ORF has been deleted (Fig. 2A) (41). The RNA2 ORF is the ORF from a PV RNA replicon (Fig. 2A) (41). The RNA2 ORF does not possess the 5′ NTR, capsid coding region, or 3′ NTR (Fig. 2A). ORF1 and ORF2 are two halves of the RNA2 ORF (Fig. 2A). In contrast to our predictions, the RNA2 ORF was resistant to cleavage by RNase L, while DJB14 RNA was readily cleaved by RNase L (Fig. 2B and C). These results indicated that the 5′ and 3′ NTRs present in DJB14 RNA were not capable of inhibiting RNase L. Likewise, these results indicated that for some reason, the RNA2 ORF was resistant to cleavage by RNase L. Because the RNA2 ORF was resistant to cleavage by RNase L, we examined two equal portions of the RNA2 ORF, i.e., ORF1 and ORF2. ORF1 was sensitive to cleavage by RNase L, while ORF2 was not (Fig. 2B and C). From these results, we speculated that a portion of the PV ORF contained in ORF2 (and the RNA2 ORF) was capable of inhibiting RNase L.

To identify the portion of PV RNA responsible for the inhibition of RNase L, we continued to test smaller and smaller subfragments of the PV ORF to identify regions of PV RNA which were resistant to cleavage by RNase L (Fig. 2D to G). ORF 2122 RNA, a 303-base fragment of PV RNA representing nt 5720 to 6023 of the 3C^{Pro} ORF, was resistant to cleavage by RNase L (Fig. 2F and G). PV RNAs containing ORF 2122 sequences were resistant to cleavage by RNase L, while PV RNAs without this region of the PV ORF were sensitive to cleavage by RNase L.

ORF 2122, a portion of the PV ORF encompassing nt 5720 to 6023, is predicted to fold into an extended RNA structure composed of several stem-loops (Fig. 3A) (46, 66). To confirm whether ORF 2122 RNA was capable of inhibiting RNase L, we assayed the ability of PV RNA to protect HCV RNA from cleavage by RNase L (Fig. 3). Increasing amounts of ORF 2122 RNA protected HCV RNA from cleavage by RNase L (Fig. 3B, lanes 2 to 4). In contrast, increasing amounts of PV ORF 2123, a fragment of PV RNA which is sensitive to cleavage by RNase L (Fig. 2F and G), did not protect HCV RNA from cleavage by RNase L (Fig. 3B, lanes 5 to 7). It is important that a molar excess of PV ORF 2122 RNA relative to 2-5A and RNase L was required for inhibition. The portions of PV RNA that resisted cleavage by RNase L were also able to protect HCV

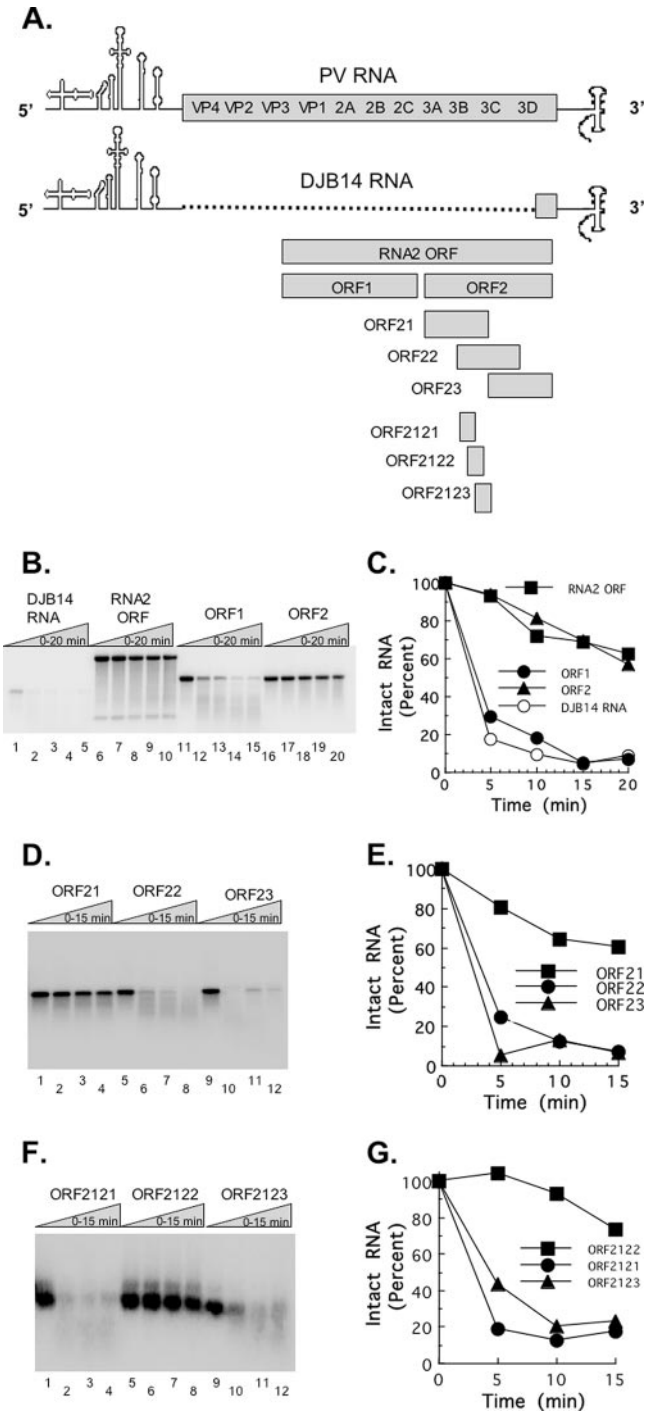

FIG. 2. Mapping of PV RNA fragments resistant to cleavage by RNase L. Fragments of PV RNA were generated by T7 transcription (A). ^{32}P-labeled PV RNAs (100 nM) were incubated for 0 to 20 min at 30°C in reaction mixtures containing purified RNase L and 2-5A (5 nM [each]). RNAs separated by electrophoresis in 1% agarose were detected by phosphorimaging (B, D, and F), and the relative amounts of intact RNA were plotted versus time of incubation (C, E, and G).

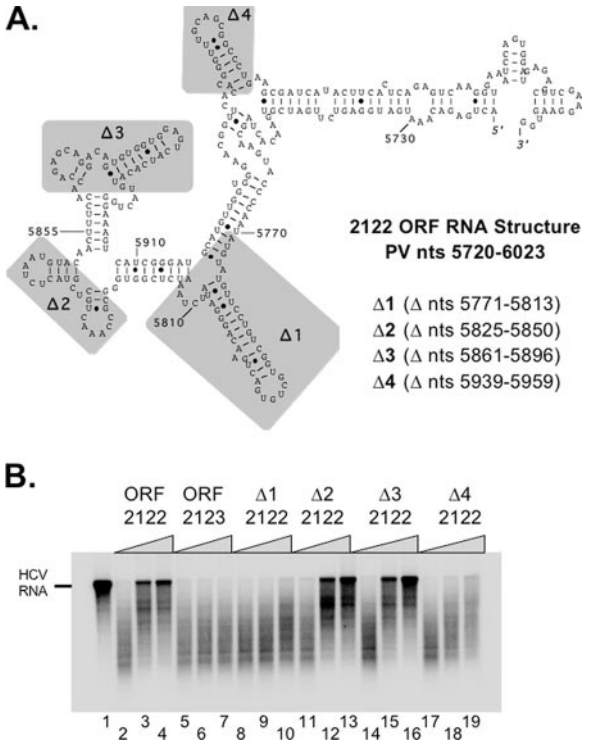

FIG. 3. PV RNA inhibits HCV RNA cleavage by RNase L, and specific deletions in ORF 2122 RNA abrogate inhibition of RNase L. (A) The structure of ORF 2122 RNA was predicted using mfold, and regions targeted for deletion are shaded in gray. (B) ^{32}P-labeled HCV RNA (100 nM) was incubated at 25°C for 0 (lane 1) or 15 (lanes 2 to 19) min in reaction mixtures containing RNase L and 2-5A (40 nM [each]). The following unlabeled PV RNAs (0, 100, or 500 nM) were included in the reaction mixtures: ORF 2122 (lanes 2 to 4), ORF 2123 (lanes 5 to 7), Δ1 ORF 2122 (lanes 8 to 10), Δ2 ORF 2122 (lanes 11 to 13), Δ3 ORF 2122 (lanes 14 to 16), and Δ4 ORF 2122 (lanes 17 to 19). ^{32}P-labeled HCV RNAs were separated by electrophoresis in 1% agarose and detected by phosphorimaging.

RNA from cleavage by RNase L. These data indicate that PV ORF 2122 RNA inhibited 2-5A-activated RNase L.

Several stem-loop structures within the ORF 2122 RNA fragment were deleted to determine their importance in the inhibition of RNase L. Δ1 2122 deleted PV nt 5771 to 5813 from ORF 2122 (Fig. 3A), Δ2 2122 deleted PV nt 5825 to 5850 from ORF 2122 (Fig. 3A), Δ3 2122 deleted PV nt 5861 to 5896 from ORF 2122 (Fig. 3A), and Δ4 2122 deleted PV nt 5939 to 5959 from ORF 2122 RNA. These deletions were designed using mfold to maintain the remaining structures of ORF 2122 beyond the deletion (46, 66; data not shown). When increasing amounts of Δ1 2122 were added to reaction mixtures containing ^{32}P-labeled HCV RNA and 2-5A-activated RNase L, HCV RNA was not protected from cleavage (Fig. 3B, lanes 8 to 10). In contrast, increasing amounts of Δ2 2122 and Δ3 2122 protected HCV RNA from cleavage by RNase L (Fig. 3B, lanes 11 to 13 and 14 to 16, respectively). Increasing amounts of Δ4 2122 were unable to protect HCV RNA from cleavage by RNase L. These results indicated that the stem-loops removed by the Δ1 and Δ4 mutations of ORF 2122 RNA are both necessary for the inhibition of RNase L, while the stem-loop RNAs deleted from the Δ2 and Δ3 RNAs are not required for the inhibition of RNase L.

PV1, the virus used in our investigations, is most closely related to type 2 and 3 PVs and several group C enteroviruses, including coxsackieviruses A11 (CA11), A17 (CA17), A20 (CA20), A13 (CA13), A21 (CA21), and A24 (CA24) (9, 30). Conserved RNA structures are not common within the ORFs of positive-strand RNA viruses (60). CRE(2C), a stem-loop RNA structure within the 2C^{ATPase} gene, is the only phylogenetically conserved RNA structure ascribed a function in the PV ORF (24, 25). Alignment of PV ORF 2122 RNA sequences with those of other PVs and group C enteroviruses revealed that the ORF 2122 RNA sequences and structures were phylogenetically conserved (Fig. 4). ORF 2122 RNA stem-loops 1 and 4, identified as being required for inhibition of RNase L (Fig. 3), are well conserved (Fig. 4A). Although the conservation of amino acid sequence can lead to some conservation of RNA sequence, the redundancy of codons for individual amino acids provides an opportunity for nucleotide variation at wobble positions of codons. The amino acid sequence of this portion of 3C protease and the wobble positions of codons (indicated by asterisks) are presented at the top of Fig. 4A. While some variation in sequence is evident at wobble positions of codons in stem-loops 1 and 4, most variation in sequence is accommodated by alternate base pairing (i.e., G-C versus G-U and A-U versus G-U) (Fig. 4A). Only 9 nt among the sequences of nine viruses aligned in Fig. 4A are not consistent with base pairing in stem-loops 1 and 4 (indicated with gray circles). Notably, the RNA sequences in the loops of stem-loops 1 and 4 are conserved and complementary (Fig. 4A, note the potential kissing interaction via complementary sequences in loops 1 and 4).

The ORF 2122 RNA sequence and structure between stem-loops 1 and 4 are also highly conserved (Fig. 4B). Only one nucleotide (in PV3) is inconsistent with this RNA structure (Fig. 4B, PV3, nt 5920). Sequence variation of the bulged nucleotide at residue 5926 does not alter the secondary structure (Fig. 4B, note the U, A, or C at residue 5926). Other sequence variations in this region, i.e., C/U changes at wobble positions, are accommodated via base pairing with G residues (Fig. 4B).

The ORF 2122 RNA sequences and structures outside the regions described above and shown in Fig. 4A and B are less conserved (data not shown) and are unnecessary for inhibition of RNase L (see below).

Functional boundaries and structural features of PV RNA associated with the inhibition of RNase L. Based on our phylogenetic analyses of sequence and structure, we designed additional mutations within ORF 2122 RNA to help define the boundaries of the important RNA elements required for inhibition of RNase L. Deletions Δ5, Δ6, Δ7, and Δ8 were engineered into ORF 2122 RNA (Fig. 5A). mfold predictions supported the illustrated structures (Fig. 5A). Based on the phylogenetic analyses and our previous data (Fig. 4), we predicted that ORF 2122 RNAs in *trans* with Δ5, Δ6, and Δ8 deletions would inhibit RNase L and that RNA with the Δ7 deletion would not inhibit RNase L. These predictions were confirmed by experimental data (Fig. 5B). As seen before, increasing amounts of ORF 2122 RNA protected ^{32}P-labeled HCV RNA from cleavage by RNase L (Fig. 5B, lanes 3 and 4).

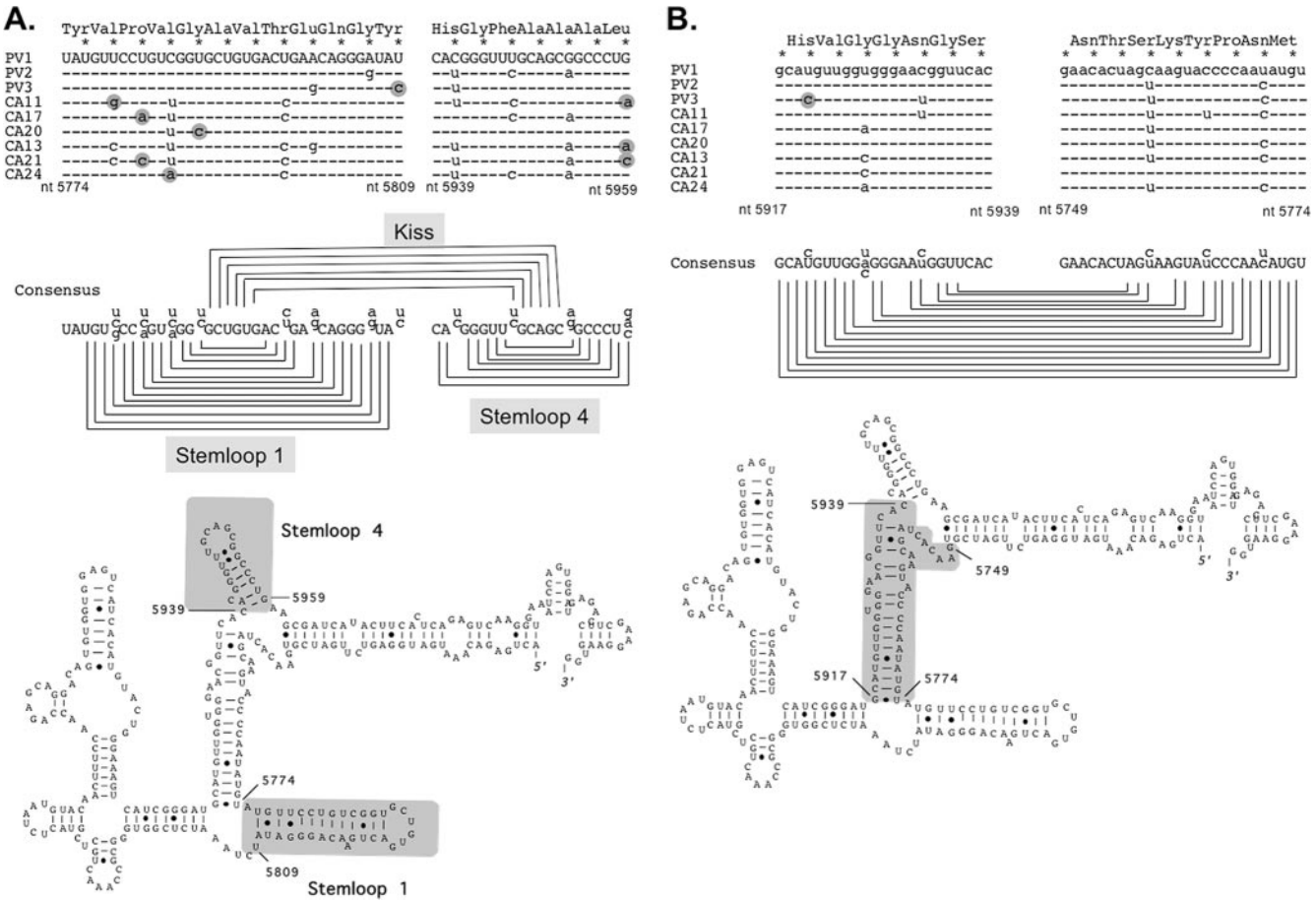

FIG. 4. Phylogenetically conserved RNA structure in the $3C^{Pro}$ ORF associated with the inhibition of RNase L. PV RNA sequences corresponding to ORF 2122 were aligned with RNA sequences of related group C enteroviruses. (A) Stem-loop 1 and stem-loop 4. (B) "Connector" region. Asterisks indicate wobble positions of codons. Nucleotides highlighted with gray circles are inconsistent with base pairing in PV ORF 2122. Viruses and nucleotide accession numbers are as follows: PV1, NC 002058; PV2, M12197; PV3, K01392; CA11, AF499636; CA17, AF499639; CA20, AF499642; CA13, AF499637; CA21, AF546702; and CA24, D90457.

ORF 2121 RNA, a PV RNA fragment susceptible to RNase L cleavage (Fig. 2F and G), was unable to protect HCV RNA from cleavage by RNase L. Increasing amounts of Δ5, Δ6, and Δ8 2122 RNAs protected HCV RNA from cleavage by RNase L (Fig. 5B), while Δ7 2122 RNA was unable to protect HCV RNA from cleavage by RNase L (Fig. 5B).

We engineered additional mutations into ORF 2122 RNA to test whether the predicted kissing interaction mediated by the complementarity of loops 1 and 4 was necessary for inhibition of RNase L (Fig. 6). Three base changes were engineered into loop 1 and loop 4 individually (loop 1 mutant and loop 4 mutant) and in combination (loop 1/4 compensatory mutant) (Fig. 6). mfold was used to confirm that these mutations would not have unintended effects on the folding of ORF 2122 RNA (data not shown). As seen before, increasing amounts of ORF 2122 RNA protected ^{32}P-labeled HCV RNA from cleavage by RNase L (Fig. 6, lanes 3 and 4), while ORF 2123 RNA, a PV RNA fragment susceptible to RNase L cleavage (Fig. 2F and G), was unable to protect HCV RNA from cleavage by RNase L. Individually, the mutations in loop 1 and loop 4 diminished the ability of ORF 2122 RNA to protect HCV RNA but did not completely debilitate ORF 2122 RNA (Fig. 6, lanes 8 to 10 and 11 to 13, respectively). In combination, these compensatory loop 1 and loop 4 mutations restored the ability of ORF 2122 RNA to protect HCV RNA from cleavage by RNase L to wild-type levels (Fig. 6, compare lanes 14 to 16 with lanes 2 to 4). These results indicate that the highly conserved RNA sequences of loops 1 and 4 are not required for inhibition of RNase L but that the complementarity of sequences in loops 1 and 4 is important in forming a functional RNA structure.

CVB3 RNA, representative of group B enteroviruses, does not resist or inhibit RNase L. Additional phylogenetic analyses and mfold analyses indicated that the conserved RNA structure of group C enteroviruses defined above was not conserved in group B enteroviruses, such as CVB3 (data not shown). Consistent with these observations, full-length infectious CVB3 RNA (12, 59) was not resistant to cleavage by RNase L like PV RNA was (Fig. 7A), and the corresponding ORF 2122 RNA region of CVB3 RNA did not protect HCV RNA from cleavage by RNase L like the ORF 2122 RNA region from PV RNA did (Fig. 7B). ORF 2122 RNA was stable in the reaction and was detected in the agarose gel by ethidium bromide staining and UV light (Fig. 7B, asterisks). Thus, the RNA-mediated inhibition of RNase L observed for group C enteroviruses

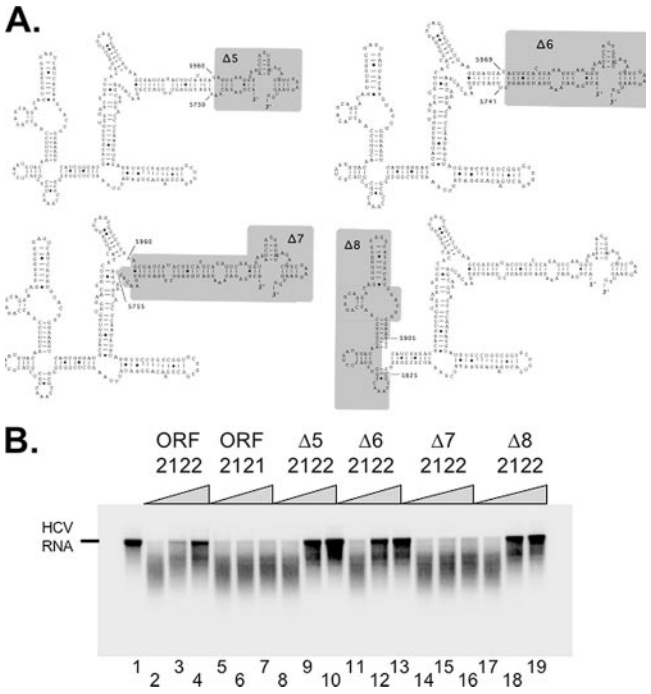

FIG. 5. Boundaries of PV RNA that inhibits RNase L activity. (A) Predicted structures of ORF 2122 RNA and regions targeted for deletion (shaded in gray). (B) ^{32}P-labeled HCV RNA (100 nM) was incubated at 30°C for 0 (lane 1) or 10 (lanes 2 to 19) min in reaction mixtures containing RNase L and 2-5A (20 nM [each]). The following unlabeled PV RNAs (0, 100, or 500 nM) were included in the reaction mixes: ORF 2122 (lanes 2 to 4), ORF 2121 (lanes 5 to 7), Δ5 ORF 2122 (lanes 8 to 10), Δ6 ORF 2122 (lanes 11 to 13), Δ7 ORF 2122 (lanes 14 to 16), and Δ8 ORF 2122 (lanes 17 to 19). ^{32}P-labeled HCV RNAs were separated by electrophoresis in 1% agarose and detected by phosphorimaging.

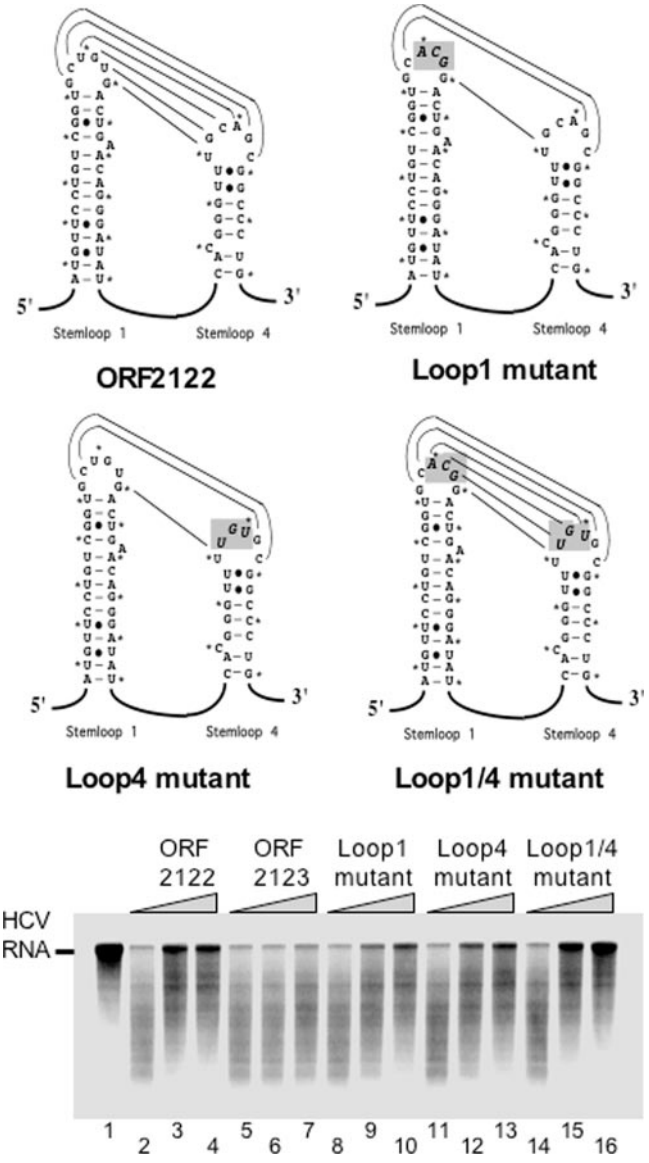

FIG. 6. Complementarity of RNA sequences in loops 1 and 4 contributes to inhibition of RNase L activity. The complementarity of loop sequences and mutations are illustrated. ^{32}P-labeled HCV RNA (100 nM) was incubated at 25°C for 0 (lane 1) or 15 (lanes 2 to 16) min in reaction mixtures containing RNase L and 2-5A (40 nM [each]). The following unlabeled PV RNAs (0, 100, or 500 nM) were included in the reaction mixes: ORF 2122 (lanes 2 to 4), ORF 2123 (lanes 5 to 7), loop 1 mutant in the context of ORF 2122 RNA (lanes 8 to 10), loop 4 mutant in the context of ORF 2122 RNA (lanes 11 to 13), and loop 1/4 compensatory mutant in the context of ORF 2122 RNA (lanes 14 to 16). ^{32}P-labeled HCV RNAs were separated by electrophoresis in 1% agarose and detected by phosphorimaging.

(such as PV) was not observed for CVB3, a group B enterovirus.

RNase L and PV replication in HeLa cells. HeLa cells stably expressing either wild-type RNase L (W12 HeLa cells) or a DN mutant RNase L (M25 HeLa cells) were used to examine the effects of RNase L on PV replication (Fig. 8). Vesicular stomatitis virus (VSV), previously reported to be unaffected by RNase L (65), was used as a control. PV and VSV grew well in both cell lines, reaching maximum titers at 6 to 8 h postadsorption (Fig. 8A). Maximum PV titers were 5.6×10^9 PFU per ml, a yield of 3,100 PFU per cell. Maximum VSV titers were 1.8×10^8 PFU per ml, a yield of 100 PFU per cell.

To determine whether RNase L was activated during the course of PV replication, we examined both the expression of RNase L (Fig. 8B) and the integrity of rRNA (Fig. 8C) in infected cells. Both wild-type RNase L (Fig. 8B, W12 HeLa cells, lanes 1 to 8) and DN RNase L (Fig. 8B, M25 HeLa cells, lanes 9 to 16) were stable throughout the course of PV infection. Two rRNA fragments characteristic of RNase L activity were clearly evident at 6 and 8 h postadsorption in PV-infected W12 HeLa cells (Fig. 8C, lanes 5 and 6, asterisks). In contrast, rRNA fragments characteristic of RNase L activity were not detected at any time in PV-infected M25 HeLa cells (Fig. 8C, lanes 7 to 11). These results are consistent with the overexpression of wild-type and DN RNase L in the respective cell lines. Because PV replicates so robustly in these cells, accumulating PV RNA was detected by ethidium bromide staining and was most noticeable at 6 h postadsorption in both W12 and M25 HeLa cells (Fig. 8C, lanes 5 and 10, arrows).

RNase L activity is correlated with larger PV plaques. PV and VSV plaque-forming efficiencies and plaque phenotypes were examined on V11 HeLa cells, W12 HeLa cells, and M25 HeLa cells (Fig. 9) (cells were fixed and stained at 3 days

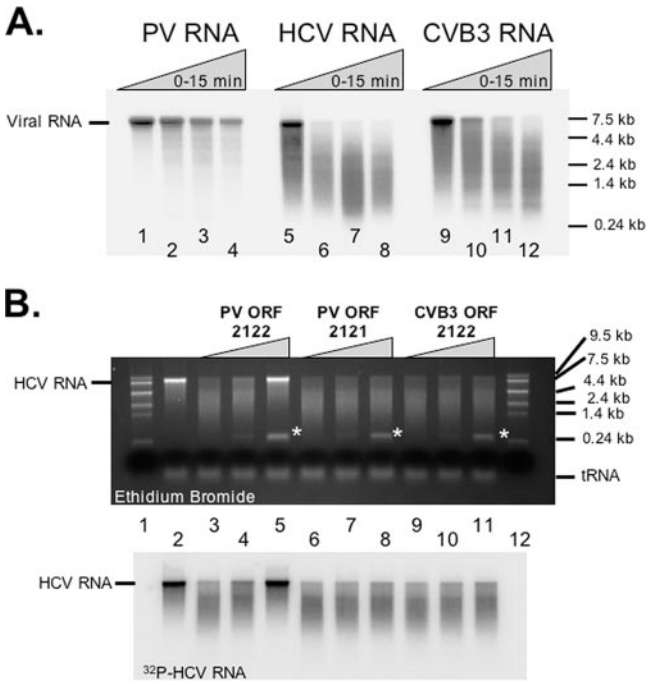

FIG. 7. CVB3 RNA does not resist or inhibit RNase L activity. (A) ^{32}P-labeled viral RNAs were assayed as described in the legend to Fig. 1. ^{32}P-labeled PV (lanes 1 to 4), HCV (lanes 5 to 8), and CVB3 (lanes 9 to 12) RNAs (100 nM) were incubated for 0, 5, 10, or 15 min at 30°C in reaction mixtures containing RNase L and 2-5A (10 nM [each]). RNAs were separated by electrophoresis in 1% agarose and detected by phosphorimaging. (B) ^{32}P-labeled HCV RNA (100 nM) was incubated at 30°C for 0 (lane 2) or 5 (lanes 3 to 11) min in reaction mixtures containing RNase L and 2-5A (10 nM [each]). The following unlabeled RNAs (0, 100, or 500 nM) were included in the reaction mixtures: PV ORF 2122 (lanes 3 to 5), PV ORF 2121 (lanes 6 to 8), and CVB3 ORF 2122 (lanes 9 to 11). RNA size markers were fractionated in lanes 1 and 12. RNAs from the reactions were separated by electrophoresis in 1% agarose and detected by ethidium bromide staining and UV light or phosphorimaging. The mobility of ORF fragments is indicated with asterisks.

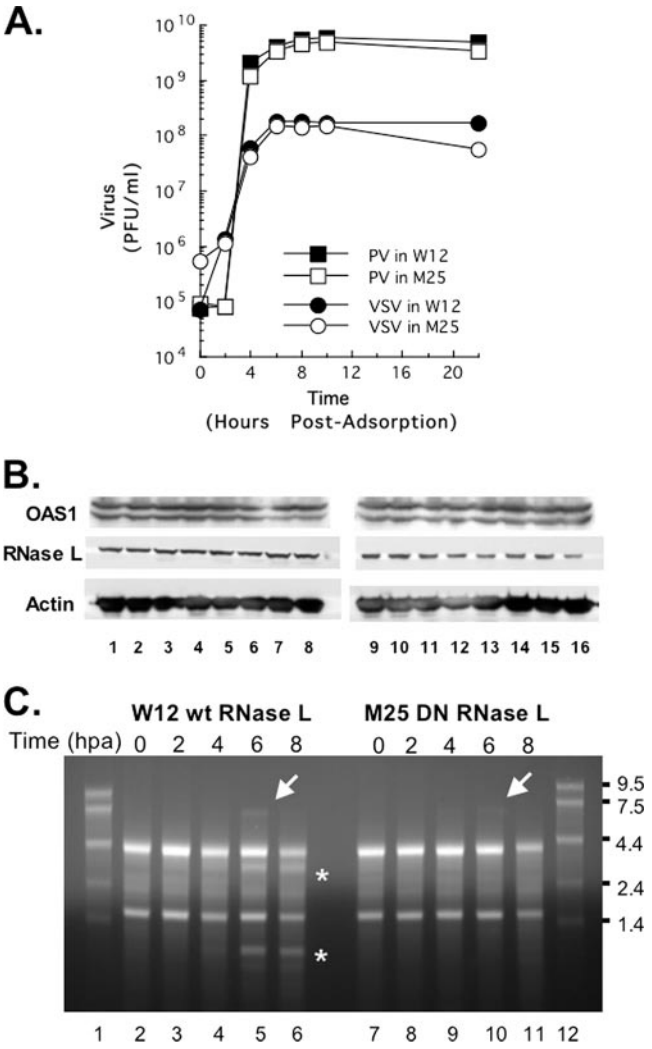

FIG. 8. One-step growth reveals activation of RNase L late during the course of PV replication. HeLa M cells overexpressing wild-type RNase L (W12) or a DN mutant RNase L (M25) were infected with wild-type PV or VSV at an MOI of 5. (A) Virus titers were determined at 0, 2, 4, 6, 8, 10, and 22 h postadsorption by plaque assay after freeze-thawing to release intracellular virus. (B) OAS1 and RNase L expression was examined by Western blotting with chemiluminescence, as described in Materials and Methods. Proteins from uninfected cells (lanes 1 and 9) and cells at 0, 1, 2, 3, 4, 5, and 6 h postadsorption (lanes 2 to 8, W12 HeLa cells; lanes 10 to 16, M25 HeLa cells) were examined. Western blotting of actin in each sample was determined as a loading control. (C) Total cellular RNA was isolated at 0, 2, 4, 6, and 8 h postadsorption (hpa) from PV-infected W12 cells (lanes 2 to 6) or PV-infected M25 cells (lanes 7 to 11). RNA size markers were fractionated in lanes 1 and 12. RNAs were separated by electrophoresis in 1% agarose, stained with ethidium bromide, and visualized with UV light. Asterisks highlight the mobility of rRNA fragments characteristic of RNase L cleavage. Arrows indicate the mobility of PV RNA.

postinfection). V11 HeLa cells express relatively small amounts of endogenous RNase L (20). V11 HeLa cells are stably transfected with empty vector rather than a vector overexpressing wild-type or mutant RNase L, as in W12 and M25 HeLa cells, respectively (see "HeLa cells expressing wild-type or DN RNase L" in Materials and Methods). PV plaques were small but easily visible in V11 HeLa cells (0.6-mm plaques), the parental HeLa cell line (Fig. 9). Expression of excess wild-type RNase L in W12 HeLa cells correlated with an increased size of PV plaques, while expression of excess DN RNase L correlated with a decreased size of PV plaques relative to those in V11 HeLa cells (Fig. 9). PV and VSV plaque-forming efficiencies were identical for the three cell lines (Fig. 9A) (an equal number of plaques was found on each cell line for a common inoculum of VSV and PV, including the extremely small PV plaques in M25 cells [Fig. 9B]). Although PV grew efficiently in both W12 and M25 HeLa cells (Fig. 8A), PV plaques were very small in M25 HeLa cells relative to those in W12 HeLa cells (Fig. 9B, see the 1-mm yellow bar for reference). These results indicate that RNase L activity may play an important role in the CPE and spread of PV from cell to cell.

PV with mutations in the RNA structure associated with inhibition of RNase L. The RNA structure associated with the inhibition of RNase L has a large number of mutable wobble positions (Fig. 10A). Mutations at the wobble positions of codons can be used to debilitate the RNA structure associated with the inhibition of RNase L without changing the amino acids encoded in this portion of the ORF. Nine wobble posi-

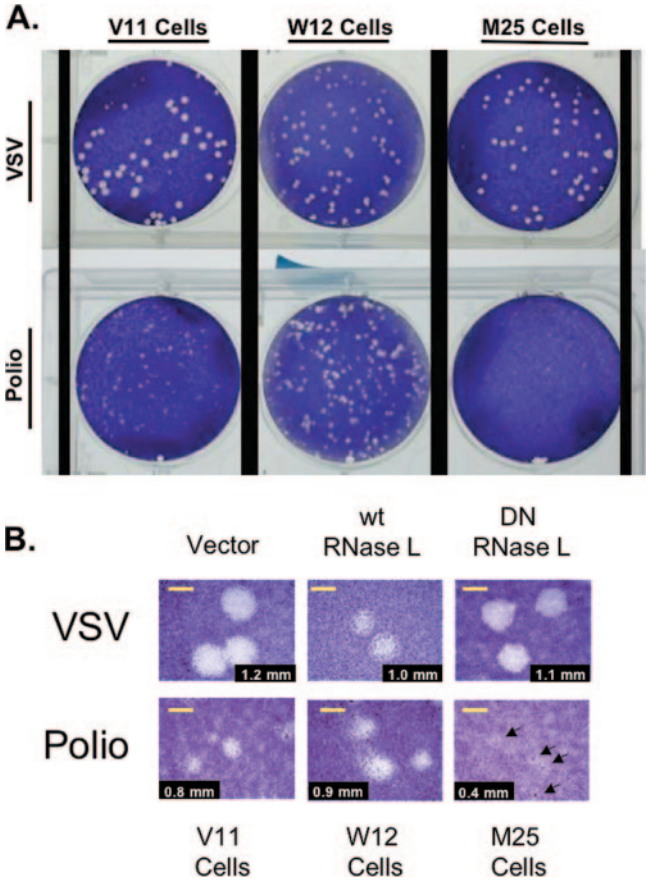

FIG. 9. Plaque phenotypes associated with RNase L. Three HeLa M cell lines stably expressing wild-type RNase L (W12), DN mutant RNase L (M25), or an empty vector (V11), as described in Materials and Methods, were infected with VSV or PV. Cells were fixed and stained with crystal violet at 3 days postinfection. (A) Monolayers without magnification. (B) Plaques observed with magnification. Yellow bars, 1 mm.

tion mutations (Fig. 10A) were engineered into ORF 2122 RNA to make ORF M1123. The same mutations were engineered into an infectious clone of PV to make the M1123 virus. ORF M1123 was not able to inhibit RNase L activity (Fig. 10B, compare lanes 8 to 10 with lanes 2 to 4). M1123 virus containing the nine wobble position mutations grew in W12 HeLa cells over several passages (Fig. 10C). Sequencing revealed that the mutations engineered into the RNA structure were maintained during replication in cells. The plaque phenotype of M1123 virus was identical to that of wild-type PV in various cell lines (HeLa M, W12 HeLa, M25 HeLa, and BSC40 cells) (data not shown). A one-step growth experiment demonstrated that M1123 PV, containing mutations in the RNA structure associated with the inhibition of RNase L, grew as efficiently as wild-type PV (Fig. 10D), consistent with the lack of observed RNase L activity in W12 HeLa cells until after virus assembly (Fig. 10E).

W12 HeLa cells were treated with interferon before infection with wild-type and mutant PVs to determine whether M1123 PV was more sensitive to interferon than wild-type PV (Fig. 11). Increasing concentrations of interferon inhibited the magnitude of PV replication, with ~1-log inhibition at 1,000 U per ml (Fig. 11, wt). M1123 PV was similarly sensitive to the inhibitory effects of interferon (Fig. 11, M1123). Thus, the inhibition of M1123 replication by interferon was not notably greater than the inhibition of wild-type PV.

DISCUSSION

Our biochemical experiments demonstrate that a previously undiscovered RNA structure in the PV ORF potently inhibits the antiviral endoribonuclease RNase L. The RNA structure is phylogenetically conserved among group C enteroviruses, as most nucleotide polymorphisms in group C enterovirus sequences are consistent with the predicted mfold structure. The only group C enteroviruses without this RNA structure, coxsackie A virus 1 (CAV1), CAV19, and CAV22, are evolutionarily distinct from the remainder of group C enteroviruses and may need to be reclassified (9). The RNA structure associated with the inhibition of RNase L is composed of two contiguous RNA sequences (PV nt 5741 to 5824 and 5906 to 5969) separated by an intervening RNA sequence (PV nt 5825 to 5905) (Fig. 3A and 10A). The intervening RNA sequence can be deleted without affecting the inhibitory action of the RNA (Fig. 5, Δ8 RNA). A notable feature of the RNA structure is the complementarity of sequences in the loops of the two stem-loops (Fig. 4A). A kissing interaction between these loops appears to be involved in the formation of a functional RNA structure (Fig. 6).

rRNA cleavage characteristic of activated RNase L was detected at relatively late times during the course of PV replication, immediately following virus assembly (Fig. 8, W12 HeLa cells at 6 h postadsorption; also see Fig. 10E). At this point in the PV replication cycle, virion RNA within virus particles would be protected from activated RNase L. RNase L activity in W12 HeLa cells did not diminish the magnitude of virus assembly, consistent with the assembly of infectious virus before the activation of RNase L (Fig. 8). Likewise, PV with mutations in the RNA structure associated with the inhibition of RNase L was not attenuated in W12 HeLa cells (Fig. 10D), consistent with the lack of rRNA cleavage characteristic of RNase L activity until after virus assembly (Fig. 10E). While rRNA cleavage is a well-defined characteristic of RNase L activity within cells, viral mRNAs are more sensitive to cleavage by RNase L than is rRNA (27). Therefore, it remains possible that RNase L activity was present in PV-infected cells at times before rRNA cleavage became apparent.

The kinetics of RNase L activation during the course of PV infection could be affected by several interrelated variables, including the amounts of OAS, viral dsRNA, and RNase L within cells. Western blots indicated that OAS and RNase L were present within HeLa cells before PV infection and that the amounts of OAS and RNase L did not change during the course of PV infection (Fig. 8B). In contrast, the amounts of viral dsRNA are expected to increase during the course of PV infection. In a typical one-step growth experiment, terminal dsRNA replicative-form (RF) products should accumulate between 1 and 5 h postadsorption, going from several dozen RFs at 1 to 2 h postinfection to 40,000 or more RFs at 4 to 6 h postinfection (35). PV dsRNA replication intermediates, like those of other viruses, are sequestered within RNA replication

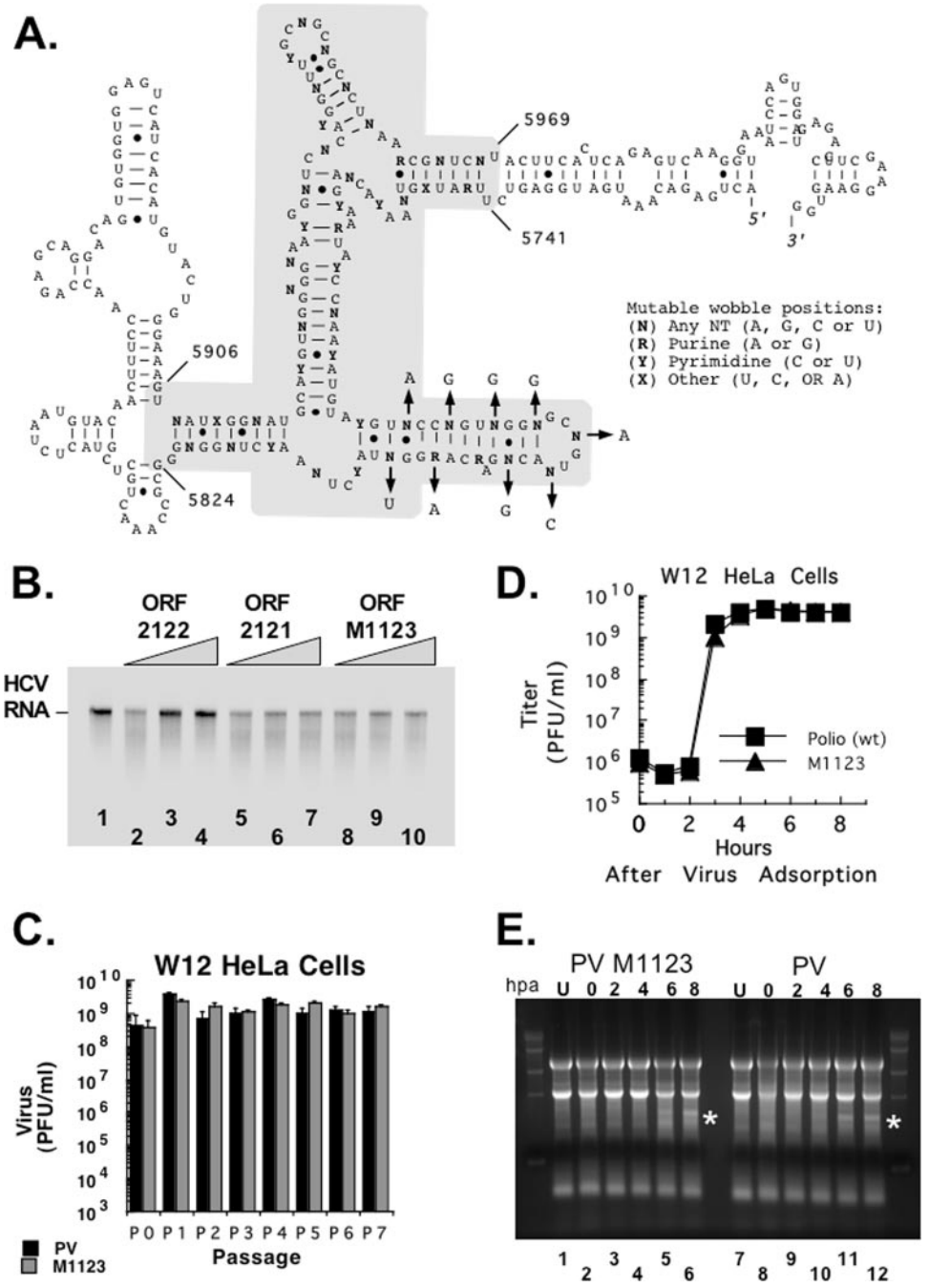

FIG. 10. PV with mutations in the RNA structure associated with the inhibition of RNase L. (A) Mutations were engineered into both ORF 2122 RNA and an infectious clone of PV at nine wobble positions within the RNA structure associated with the inhibition of RNase L. (B) HCV RNA protection assay as described in the legend to Fig. 3. ^{32}P-labeled HCV RNA (100 nM) was incubated at 30°C for 0 (lane 1) or 5 (lanes 2 to 10) min in reaction mixtures containing RNase L and 2-5A (10 nM [each]). The following unlabeled RNAs (0, 100, or 500 nM) were included in the reaction mixtures: PV ORF 2122 (lanes 2 to 4), PV ORF 2121 (lanes 5 to 7), and M1123 ORF with nine wobble position mutations in the context of ORF 2122 RNA (lanes 8 to 10). ^{32}P-labeled HCV RNAs were separated by electrophoresis and detected by phosphorimaging. (C) Wild-type PV RNA and M1123 PV RNA containing nine wobble position mutations, as illustrated, were transfected into W12 HeLa cells. Viruses obtained at 24 h posttransfection were titrated (P_0) and passaged seven times at an MOI of 0.01 in W12 HeLa cells. The P5 virus was sequenced and found to have maintained the nine mutations engineered into wobble positions. (D) One-step growth of wild-type PV and PV M1123 in W12 HeLa cells. W12 HeLa M cells overexpressing wild-type RNase L were infected with wild-type PV or PV M1123 at an MOI of 5. Virus titers were determined at 0, 1, 2, 3, 4, 5, 6, 7, and 8 h postadsorption by plaque assay after freeze-thawing cells three times to release intracellular virus. (E) Total cellular RNA was isolated from uninfected W12 cells (lanes 1 and 7), PV M1123-infected W12 cells at 0, 2, 4, 6, and 8 h postadsorption (lanes 2 to 6), or PV wild-type-infected cells at 0, 2, 4, 6, and 8 h postadsorption (lanes 8 to 12). RNAs were separated by electrophoresis in 1% agarose, stained with ethidium bromide, and visualized with UV light. Asterisks highlight the mobility of rRNA fragments characteristic of RNase L cleavage.

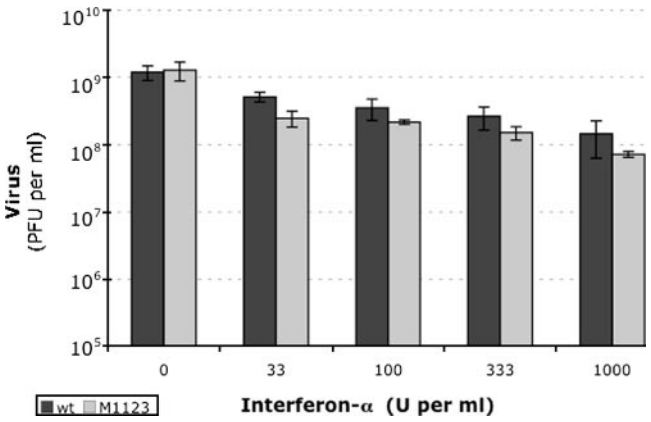

FIG. 11. Interferon inhibits the magnitude of wild-type and mutant PV replication. W12 HeLa cells were treated for 18 h with the indicated concentrations of universal type 1 interferon (PBL Biomedical Laboratories). Following interferon treatment, cells were infected with wild-type or M1123 mutant PV at an MOI of 0.01 PFU per cell. Virus titers were determined at 20 h postinfection by plaque assay after freeze-thawing cells three times to release intracellular virus.

complexes early during infection, potentially precluding activation of 2-5 OASs until the release of the dsRNAs from replication complexes (3, 8). Over time, as membranous RNA replication complexes disassemble or decay, viral dsRNAs within the replication complexes would be released and accumulate in the cytoplasm (35). The kinetics by which PV dsRNAs are released from membranous RNA replication complexes have not been reported. Our results suggest that PV dsRNAs/RFs do not activate OAS until virus assembly is reaching completion (at ~6 h postadsorption/7 h postinfection) (Fig. 8).

In addition to the factors described above, there are several other factors that contribute to the regulation of RNase L activity in cells. 2-5 OAS has a weak RNA binding domain, so relatively large amounts of dsRNA are required for activation relative to those for other dsRNA-activated antiviral proteins, such as protein kinase R (PKR) (28). 5′-Phosphorylated 2-5A trimers must accumulate to functional levels following activation of OAS. 5′-Phosphatase and 2′-phosphodiesterase are enzymes that inactivate and degrade 2-5A, negatively affecting 2-5A accumulation (33, 37). An RNase L inhibitor may also affect the kinetics of RNase L activation (45). Finally, packaging of nascent viral RNAs late during the course of infection would preclude their contribution to inhibition of RNase L because virion RNAs sequestered within capsid proteins could not bind RNase L. Thus, a series of events could lead to the activation of RNase L late during the course of PV infection.

Activation of RNase L as virus assembly reaches completion, perhaps in concert with other dsRNA-activated pathways, could be an important, normal aspect of PV replication. Nascent PV assembles within the cytoplasm of infected cells. CPE associated with dsRNA accumulation and other viral insults to the cell may lead to a loss of membrane integrity and to virus release (35). Uptake of trypan blue by apoptotic HeLa cells late during PV infection (after 10 h postinfection) is consistent with this possibility (49). Vadim Agol et al. developed a helpful theoretical framework regarding cell death associated with PV infection (1, 58). When PV replication is robust (as in HeLa cells), cells die predominantly via delayed apoptotic death (49). Alternatively, when PV replication is less robust, due to infection under less permissive conditions, cells die earlier via apoptotic pathways (2). This general framework holds true in most circumstances, including PV infection of primary mouse embryo fibroblasts and primary neurons from human poliovirus receptor transgenic mice (17). RNase L, which was activated as virus assembly neared completion, is known to be proapoptotic (39, 65). Furthermore, RNase L contributes to the apoptotic death of PV-infected cells (10), consistent with increased plaque sizes associated with RNase L activation following virus assembly (Fig. 8 and 9). Thus, rather than inhibiting PV replication, as concluded by Castelli et al. (10), RNase L-mediated apoptotic death may be a feature of cellular metabolism coopted by PV to facilitate CPE and virus release.

Interferon, which activates the expression of 2-5 OASs, would be expected to increase the antiviral activity of RNase L during infection (55). We tested this possibility in HeLa cells (Fig. 11). Although interferon inhibited PV replication in a dose-dependent manner, the magnitude of inhibition was not notably higher for the mutant PV M1123 than for wild-type PV (Fig. 11). Interferon is clearly important in the pathogenesis of PV infections in vivo (31). Antiviral states regulated by alpha/beta interferon receptors regulate tissue tropism and appear to be more active in vivo than in tissue culture (63). Because PV M1123 grew as well as wild-type PV under the conditions examined, it remains to be determined how the RNA structure associated with the inhibition of RNase L contributes to PV replication and pathogenesis.

Intriguingly, RNA-mediated countermeasures of innate immunity have been described for two DNA viruses, namely, Epstein-Barr virus and adenoviruses. Epstein-Barr virus expresses EBER1 RNA and EBER2 RNA. EBER RNAs appear to counteract PKR (14, 15, 53), an interferon-regulated and dsRNA-activated antiviral protein, and may also affect host proteins other than PKR (38). VAI and VAII RNAs are abundantly expressed adenovirus RNAs that appear to counteract both PKR (13, 32, 42, 48) and RNA interference (4, 40). EBER RNAs may functionally substitute for adenovirus VA RNAs (7). We have not observed any similarity of sequence or structure between EBER RNAs (23) or VA RNAs (42–44) and the PV RNA structure that inhibits RNase L.

PV is targeted for eradication by the World Health Organization, but social, economic, political, and scientific problems have made this goal elusive (11, 29, 56; www.polioeradication.org). It will be important to determine whether mutations in the RNA structure associated with the inhibition of RNase L attenuate PV or other group C enteroviruses in vivo. Mutations within viral RNA structures that counteract innate immune pathways, such as RNase L, could prove advantageous in vaccines, especially if such mutations attenuate virus replication preferentially in vivo rather than in tissue culture. Sequence analyses indicate that the RNA structure associated with the inhibition of RNase L is intact in the attenuated Sabin vaccine strains (data not shown). New PV vaccines may need to be considered, especially if circulating Sabin vaccine-derived PVs prove problematic in the eradication campaign, as predicted (19, 34).

ACKNOWLEDGMENTS

We thank Charlie Rice (Rockefeller University) for HCV cDNA and Nora Chapman (University of Nebraska) for CVB3 cDNA. Kevin Durand and Christopher Washenberger provided technical assistance.

This work was supported by the American Cancer Society (RSG-02-063-01 to D.J.B.) and the National Cancer Institute (CA44059 to R.H.S.).

REFERENCES

1. **Agol, V. I., G. A. Belov, K. Bienz, D. Egger, M. S. Kolesnikova, N. T. Raikhlin, L. I. Romanova, E. A. Smirnova, and E. A. Tolskaya.** 1998. Two types of death of poliovirus-infected cells: caspase involvement in the apoptosis but not cytopathic effect. Virology **252:**343–353.
2. **Agol, V. I., G. A. Belov, K. Bienz, D. Egger, M. S. Kolesnikova, L. I. Romanova, L. V. Sladkova, and E. A. Tolskaya.** 2000. Competing death programs in poliovirus-infected cells: commitment switch in the middle of the infectious cycle. J. Virol. **74:**5534–5541.
3. **Ahlquist, P.** 2006. Parallels among positive-strand RNA viruses, reverse-transcribing viruses and double-stranded RNA viruses. Nat. Rev. Microbiol. **4:**371–382.
4. **Andersson, M. G., P. C. Haasnoot, N. Xu, S. Berenjian, B. Berkhout, and G. Akusjarvi.** 2005. Suppression of RNA interference by adenovirus virus-associated RNA. J. Virol. **79:**9556–9565.
5. **Barton, D. J., B. J. O'Donnell, and J. B. Flanegan.** 2001. 5′ cloverleaf in poliovirus RNA is a cis-acting replication element required for negative-strand synthesis. EMBO J. **20:**1439–1448.
6. **Bayliss, C. D., and R. C. Condit.** 1993. Temperature-sensitive mutants in the vaccinia virus A18R gene increase double-stranded RNA synthesis as a result of aberrant viral transcription. Virology **194:**254–262.
7. **Bhat, R. A., and B. Thimmappaya.** 1983. Two small RNAs encoded by Epstein-Barr virus can functionally substitute for the virus-associated RNAs in the lytic growth of adenovirus 5. Proc. Natl. Acad. Sci. USA **80:**4789–4793.
8. **Bolten, R., D. Egger, R. Gosert, G. Schaub, L. Landmann, and K. Bienz.** 1998. Intracellular localization of poliovirus plus- and minus-strand RNA visualized by strand-specific fluorescent in situ hybridization. J. Virol. **72:**8578–8585.
9. **Brown, B., M. S. Oberste, K. Maher, and M. A. Pallansch.** 2003. Complete genomic sequencing shows that polioviruses and members of human enterovirus species C are closely related in the noncapsid coding region. J. Virol. **77:**8973–8984.
10. **Castelli, J. C., B. A. Hassel, K. A. Wood, X. L. Li, K. Amemiya, M. C. Dalakas, P. F. Torrence, and R. J. Youle.** 1997. A study of the interferon antiviral mechanism: apoptosis activation by the 2-5A system. J. Exp. Med. **186:**967–972.
11. **Centers for Disease Control and Prevention.** 2005. Progress toward poliomyelitis eradication—poliomyelitis outbreak in Sudan, 2004. Morb. Mortal. Wkly. Rep. **54:**97–99.
12. **Chapman, N. M., Z. Tu, S. Tracy, and C. J. Gauntt.** 1994. An infectious cDNA copy of the genome of a non-cardiovirulent coxsackievirus B3 strain: its complete sequence analysis and comparison to the genomes of cardiovirulent coxsackieviruses. Arch. Virol. **135:**115–130.
13. **Clarke, P. A., T. Pe'ery, Y. Ma, and M. B. Mathews.** 1994. Structural features of adenovirus 2 virus-associated RNA required for binding to the protein kinase DAI. Nucleic Acids Res. **22:**4364–4374.
14. **Clarke, P. A., M. Schwemmle, J. Schickinger, K. Hilse, and M. J. Clemens.** 1991. Binding of Epstein-Barr virus small RNA EBER-1 to the double-stranded RNA-activated protein kinase DAI. Nucleic Acids Res. **19:**243–248.
15. **Clarke, P. A., N. A. Sharp, and M. J. Clemens.** 1990. Translational control by the Epstein-Barr virus small RNA EBER-1. Reversal of the double-stranded RNA-induced inhibition of protein synthesis in reticulocyte lysates. Eur. J. Biochem. **193:**635–641.
16. **Cohrs, R. J., R. C. Condit, R. F. Pacha, C. L. Thompson, and O. K. Sharma.** 1989. Modulation of ppp(A2′p)nA-dependent RNase by a temperature-sensitive mutant of vaccinia virus. J. Virol. **63:**948–951.
17. **Daley, J. K., L. A. Gechman, J. Skipworth, and G. F. Rall.** 2005. Poliovirus replication and spread in primary neuron cultures. Virology **340:**10–20.
18. **Desai, S. Y., and G. C. Sen.** 1997. Effects of varying lengths of double-stranded RNA on binding and activation of 2′-5′-oligoadenylate synthetase. J. Interferon Cytokine Res. **17:**531–536.
19. **Diamond, B.** 2005. Global polio campaign doomed to fail, experts warn. Nat. Med. **11:**1260.
20. **Dong, B., M. Niwa, P. Walter, and R. H. Silverman.** 2001. Basis for regulated RNA cleavage by functional analysis of RNase L and Ire1p. RNA **7:**361–373.
21. **Dong, B., and R. H. Silverman.** 1995. 2-5A-dependent RNase molecules dimerize during activation by 2-5A. J. Biol. Chem. **270:**4133–4137.
22. **Floyd-Smith, G., E. Slattery, and P. Lengyel.** 1981. Interferon action: RNA cleavage pattern of a (2′-5′)oligoadenylate-dependent endonuclease. Science **212:**1030–1032.
23. **Glickman, J. N., J. G. Howe, and J. A. Steitz.** 1988. Structural analyses of EBER1 and EBER2 ribonucleoprotein particles present in Epstein-Barr virus-infected cells. J. Virol. **62:**902–911.
24. **Goodfellow, I., Y. Chaudhry, A. Richardson, J. Meredith, J. W. Almond, W. Barclay, and D. J. Evans.** 2000. Identification of a *cis*-acting replication element within the poliovirus coding region. J. Virol. **74:**4590–4600.
25. **Goodfellow, I. G., D. Kerrigan, and D. J. Evans.** 2003. Structure and function analysis of the poliovirus cis-acting replication element (CRE). RNA **9:**124–137.
26. **Han, J. Q., and D. J. Barton.** 2002. Activation and evasion of the antiviral 2′-5′ oligoadenylate synthetase/ribonuclease L pathway by hepatitis C virus mRNA. RNA **8:**512–525.
27. **Han, J. Q., G. Wroblewski, Z. Xu, R. H. Silverman, and D. J. Barton.** 2004. Sensitivity of hepatitis C virus RNA to the antiviral enzyme ribonuclease L is determined by a subset of efficient cleavage sites. J. Interferon Cytokine Res. **24:**664–676.
28. **Hartmann, R., J. Justesen, S. N. Sarkar, G. C. Sen, and V. C. Yee.** 2003. Crystal structure of the 2′-specific and double-stranded RNA-activated interferon-induced antiviral protein 2′-5′-oligoadenylate synthetase. Mol. Cell **12:**1173–1185.
29. **Heymann, D. L., R. W. Sutter, and R. B. Aylward.** 2005. A global call for new polio vaccines. Nature **434:**699–700.
30. **Hyypia, T., T. Hovi, N. J. Knowles, and G. Stanway.** 1997. Classification of enteroviruses based on molecular and biological properties. J. Gen. Virol. **78:**1–11.
31. **Ida-Hosonuma, M., T. Iwasaki, T. Yoshikawa, N. Nagata, Y. Sato, T. Sata, M. Yoneyama, T. Fujita, C. Taya, H. Yonekawa, and S. Koike.** 2005. The alpha/beta interferon response controls tissue tropism and pathogenicity of poliovirus. J. Virol. **79:**4460–4469.
32. **Jimenez-Garcia, L. F., S. R. Green, M. B. Mathews, and D. L. Spector.** 1993. Organization of the double-stranded RNA-activated protein kinase DAI and virus-associated VA RNAI in adenovirus-2-infected HeLa cells. J. Cell Sci. **106:**11–22.
33. **Johnston, M. I., and W. G. Hearl.** 1987. Purification and characterization of a 2′-phosphodiesterase from bovine spleen. J. Biol. Chem. **262:**8377–8382.
34. **Kew, O. M., R. W. Sutter, E. M. de Gourville, W. R. Dowdle, and M. A. Pallansch.** 2005. Vaccine-derived polioviruses and the endgame strategy for global polio eradication. Annu. Rev. Microbiol. **59:**587–635.
35. **Koch, F., and G. Koch.** 1985. The molecular biology of poliovirus. Springer-Verlag, New York, NY.
36. **Kolykhalov, A. A., E. V. Agapov, K. J. Blight, K. Mihalik, S. M. Feinstone, and C. M. Rice.** 1997. Transmission of hepatitis C by intrahepatic inoculation with transcribed RNA. Science **277:**570–574.
37. **Kubota, K., K. Nakahara, T. Ohtsuka, S. Yoshida, J. Kawaguchi, Y. Fujita, Y. Ozeki, A. Hara, C. Yoshimura, H. Furukawa, H. Haruyama, K. Ichikawa, M. Yamashita, T. Matsuoka, and Y. Iijima.** 2004. Identification of 2′-phosphodiesterase, which plays a role in the 2-5A system regulated by interferon. J. Biol. Chem. **279:**37832–37841.
38. **Laing, K. G., A. Elia, I. Jeffrey, V. Matys, V. J. Tilleray, B. Souberbielle, and M. J. Clemens.** 2002. In vivo effects of the Epstein-Barr virus small RNA EBER-1 on protein synthesis and cell growth regulation. Virology **297:**253–269.
39. **Li, G., Y. Xiang, K. Sabapathy, and R. H. Silverman.** 2004. An apoptotic signaling pathway in the interferon antiviral response mediated by RNase L and c-Jun NH_2-terminal kinase. J. Biol. Chem. **279:**1123–1131.
40. **Lu, S., and B. R. Cullen.** 2004. Adenovirus VA1 noncoding RNA can inhibit small interfering RNA and microRNA biogenesis. J. Virol. **78:**12868–12876.
41. **Lyons, T., K. E. Murray, A. W. Roberts, and D. J. Barton.** 2001. Poliovirus 5′-terminal cloverleaf RNA is required in *cis* for VPg uridylylation and the initiation of negative-strand RNA synthesis. J. Virol. **75:**10696–10708.
42. **Ma, Y., and M. B. Mathews.** 1993. Comparative analysis of the structure and function of adenovirus virus-associated RNAs. J. Virol. **67:**6605–6617.
43. **Ma, Y., and M. B. Mathews.** 1996. Secondary and tertiary structure in the central domain of adenovirus type 2 VA RNA I. RNA **2:**937–951.
44. **Ma, Y., and M. B. Mathews.** 1996. Structure, function, and evolution of adenovirus-associated RNA: a phylogenetic approach. J. Virol. **70:**5083–5099.
45. **Martinand, C., T. Salehzada, M. Silhol, B. Lebleu, and C. Bisbal.** 1998. The RNase L inhibitor (RLI) is induced by double-stranded RNA. J. Interferon Cytokine Res. **18:**1031–1038.
46. **Mathews, D. H., J. Sabina, M. Zuker, and D. H. Turner.** 1999. Expanded sequence dependence of thermodynamic parameters improves prediction of RNA secondary structure. J. Mol. Biol. **288:**911–940.
47. **Player, M. R., and P. F. Torrence.** 1998. The 2-5A system: modulation of viral and cellular processes through acceleration of RNA degradation. Pharmacol. Ther. **78:**55–113.
48. **Rice, A. P., M. Kostura, and M. B. Mathews.** 1989. Identification of a 90-kDa polypeptide which associates with adenovirus VA RNAI and is phosphorylated by the double-stranded RNA-dependent protein kinase. J. Biol. Chem. **264:**20632–20637.
49. **Romanova, L. I., G. A. Belov, P. V. Lidsky, E. A. Tolskaya, M. S. Kolesnikova, A. G. Evstafieva, A. B. Vartapetian, D. Egger, K. Bienz, and V. I. Agol.**

2005. Variability in apoptotic response to poliovirus infection. Virology **331:** 292–306.

50. **Rusch, L., B. Dong, and R. H. Silverman.** 2001. Monitoring activation of ribonuclease L by 2′,5′-oligoadenylates using purified recombinant enzyme and intact malignant glioma cells. Methods Enzymol. **342:**10–20.
51. **Sarnow, P.** 1989. Role of 3′-end sequences in infectivity of poliovirus transcripts made in vitro. J. Virol. **63:**467–470.
52. **Scherbik, S. V., J. M. Paranjape, B. M. Stockman, R. H. Silverman, and M. A. Brinton.** 2006. RNase L plays a role in the antiviral response to West Nile virus. J. Virol. **80:**2987–2999.
53. **Sharp, T. V., M. Schwemmle, I. Jeffrey, K. Laing, H. Mellor, C. G. Proud, K. Hilse, and M. J. Clemens.** 1993. Comparative analysis of the regulation of the interferon-inducible protein kinase PKR by Epstein-Barr virus RNAs EBER-1 and EBER-2 and adenovirus VAI RNA. Nucleic Acids Res. **21:** 4483–4490.
54. **Silverman, R. H., B. Dong, R. K. Maitra, M. R. Player, and P. F. Torrence.** 2000. Selective RNA cleavage by isolated RNase L activated with 2-5A antisense chimeric oligonucleotides. Methods Enzymol. **313:**522–533.
55. **Silverman, R. H., J. J. Skehel, T. C. James, D. H. Wreschner, and I. M. Kerr.** 1983. rRNA cleavage as an index of ppp(A2′p)nA activity in interferon-treated encephalomyocarditis virus-infected cells. J. Virol. **46:**1051–1055.
56. **Soares, C.** 2005. Polio postponed. Politics slow polio's eradication—and cause it to spread. Sci. Am. **292:**8–9.
57. **Tanaka, N., M. Nakanishi, Y. Kusakabe, Y. Goto, Y. Kitade, and K. T. Nakamura.** 2004. Structural basis for recognition of 2′,5′-linked oligoadenylates by human ribonuclease L. EMBO J. **23:**3929–3938.
58. **Tolskaya, E. A., L. I. Romanova, M. S. Kolesnikova, T. A. Ivannikova, E. A. Smirnova, N. T. Raikhlin, and V. I. Agol.** 1995. Apoptosis-inducing and apoptosis-preventing functions of poliovirus. J. Virol. **69:**1181–1189.
59. **Tu, Z., N. M. Chapman, G. Hufnagel, S. Tracy, J. R. Romero, W. H. Barry, L. Zhao, K. Currey, and B. Shapiro.** 1995. The cardiovirulent phenotype of coxsackievirus B3 is determined at a single site in the genomic 5′ nontranslated region. J. Virol. **69:**4607–4618.
60. **Witwer, C., S. Rauscher, I. L. Hofacker, and P. F. Stadler.** 2001. Conserved RNA secondary structures in Picornaviridae genomes. Nucleic Acids Res. **29:**5079–5089.
61. **Wreschner, D. H., T. C. James, R. H. Silverman, and I. M. Kerr.** 1981. Ribosomal RNA cleavage, nuclease activation and 2-5A(ppp(A2′p)nA) in interferon-treated cells. Nucleic Acids Res. **9:**1571–1581.
62. **Wreschner, D. H., J. W. McCauley, J. J. Skehel, and I. M. Kerr.** 1981. Interferon action—sequence specificity of the ppp(A2′p)nA-dependent ribonuclease. Nature **289:**414–417.
63. **Yoshikawa, T., T. Iwasaki, M. Ida-Hosonuma, M. Yoneyama, T. Fujita, H. Horie, M. Miyazawa, S. Abe, B. Simizu, and S. Koike.** 2006. Role of the alpha/beta interferon response in the acquisition of susceptibility to poliovirus by kidney cells in culture. J. Virol. **80:**4313–4325.
64. **Zhou, A., R. J. Molinaro, K. Malathi, and R. H. Silverman.** 2005. Mapping of the human RNASEL promoter and expression in cancer and normal cells. J. Interferon Cytokine Res. **25:**595–603.
65. **Zhou, A., J. Paranjape, T. L. Brown, H. Nie, S. Naik, B. Dong, A. Chang, B. Trapp, R. Fairchild, C. Colmenares, and R. H. Silverman.** 1997. Interferon action and apoptosis are defective in mice devoid of 2′,5′-oligoadenylate-dependent RNase L. EMBO J. **16:**6355–6363.
66. **Zuker, M.** 2003. Mfold web server for nucleic acid folding and hybridization prediction. Nucleic Acids Res. **31:**3406–3415.